DOI: 10.1002/ejp.1864

EJP European Journal of Pain

ORIGINAL ARTICLE

Central sensitization of dorsal root potentials and dorsal root reflexes: An in vitro study in the mouse spinal cord.

Jorge Vicente-Baz | **Jose Antonio Lopez-Garcia** | **Ivan Rivera-Arconada**

Department of Systems Biology (Physiology), Universidad de Alcala, Alcala de Henares, Madrid, Spain

Correspondence
Ivan Rivera Arconada, Department of Biología de Sistemas (Área Fisiología), Edificio de Medicina, Campus Universitario, Universidad de Alcalá, Alcalá de Henares, 28805 Madrid, Spain.
Email: ivan.rivera@uah.es

Funding information
This work was supported by the Spanish Ministry of Economy and Competitiveness (Grant No. SAF2016-77585-R). Jorge Vicente-Baz enjoyed a PhD grant of the University of Alcala.

Abstract

Background: Axo-axonic contacts onto central terminals of primary afferents modulate sensory inputs to the spinal cord. These contacts produce primary afferent depolarization (PAD), which serves as a mechanism for presynaptic inhibition, and also produce dorsal root reflexes (DRRs), which may regulate the excitability of peripheral terminals and second order neurons. We aimed to identify changes in these responses as a consequence of peripheral inflammation.

Methods: *In vitro* spinal cord recordings of spontaneous activities in dorsal and ventral roots were performed in control mice and following paw inflammation. We also used pharmacological assays to define the neurotransmitter systems implicated in such responses.

Results: Paw inflammation increased the frequency and amplitude of spontaneous dorsal root depolarizations, the occurrence of DRRs and the amplitude of ventral roots depolarizations. PAD was classified in two different patterns based on their relation to ventral activity: time-locked and independent events. Both patterns increased in amplitude after paw inflammation, and independent events also increased in frequency. The circuits that were responsible for this activity implicated both glutamatergic and GABAergic transmission. Adrenergic modulation differentially affected both types of PAD, and this modulation changed after paw inflammation.

Conclusions: Our findings suggest the existence of independent spinal circuits at the origin of PAD and DRRs. Inflammation modulates these circuits differentially, unveiling varied mechanisms of spinal sensitization. This *in vitro* approach provides an isolated model for the study of the mechanisms of central sensitization and for the performance of pharmacological assays with the purpose of identifying and testing novel antinociceptive targets.

Significance: Spinal circuits modulate activity of primary afferents acting on central terminals. Under *in vitro* conditions, dorsal roots show spontaneous activity in the form of depolarizations and action potentials. Our findings are consistent with the existence of several independent generator circuits. Experimental paw inflammation reduced mechanical withdrawal threshold and significantly

increased the spontaneous activity of dorsal roots, which may be secondary to an enhanced output of spinal generators. This can be considered as a novel sign of central sensitization.

1 | INTRODUCTION

Inside the spinal cord, central terminals of primary afferents receive axo-axonic contacts that regulate their excitability, modulating neurotransmitters' release and the entry of somatosensory information from the periphery (Rudomin & Schmidt, 1999). Circuits responsible for presynaptic contacts are formed by interneurons located in the spinal cord that are activated by segmental and descending inputs (Jimenez et al., 1987; Rudomin, 1990). Axo-axonic contacts are produced by GABAergic neurons, and identified subpopulations are implicated in inhibiting the information coming into the cord through specific afferents (Barber et al., 1978; Boyle et al., 2019; Fink et al., 2014). Opening of GABA-A receptors produces depolarization by chloride ions' efflux, due to the particular chloride gradient present in primary afferent terminals (Price et al., 2009). Transmitter release from afferents can be reduced by inactivation of voltage-dependent sodium channels, which may alter action potential amplitude and shape at the terminal, and/or inactivation of calcium channels, reducing calcium entry into the presynaptic terminal (French et al., 2006; Rudomin & Schmidt, 1999). In addition, action potential amplitude can also be reduced by an increase in membrane conductance or shunting caused by GABA-A receptors' opening (French et al., 2006). Additional neurotransmitters and modulators may shape presynaptic control of peripheral inputs. Among others, the implication of NMDA and GABA-B receptors, as well as serotonin, noradrenaline and opiates has been described (Willis, 1999; Zimmerman et al., 2019).

Presynaptic activity onto central terminals can also elicit action potentials that may travel along the afferents in antidromic direction towards the periphery (dorsal root reflexes-DRRs-). DRRs have been reported in cutaneous and muscle afferents during fictive locomotion (Dubuc et al., 1985; Gossard et al., 1999), as well as in nociceptive fibres after peripheral inflammation (Lin et al., 2000; Sluka et al., 1995). DRRs in stretch-sensitive muscle afferents interfere with the mechanisms of spike generation in peripheral receptors, altering the discharge of action potentials (Gossard et al., 1999). In nociceptive afferents, DRRs may invade peripheral terminals releasing proinflammatory mediators and leading to neurogenic inflammation and nociceptor sensitization (Willis, 1999). In addition, it has been postulated that DRRs elicited by presynaptic contacts onto primary afferent must also travel in orthodromic direction. If such activity affected nociceptive primary afferents, this would lead to the activation of nociceptive pathways (Cervero & Laird, 1996; Guo & Hu, 2014).

Here, we aimed to study changes in the spinal circuits implicated in the generation of PAD and DRRs due to a sensitization process. For this purpose, we used a model of peripheral inflammation and *in vitro* electrophysiological recordings of spontaneous PAD and DRRs reflecting the intrinsic activity of these circuits. Spontaneous activity in motor neurons was simultaneously recorded for comparison on the effects of inflammation in the motor output of the cord and for studying sensory-motor communication. The influence of the main excitatory and inhibitory neurotransmitters and the descending adrenergic pathway on the spinal circuits responsible for spontaneous activity was also tested by pharmacological assays. This work provides insights into the functioning of the spinal circuits mediating PAD and DRRs and their modifications after peripheral inflammation.

2 | MATERIALS AND METHODS

Experiments were performed on a total of 97 CD1 mice of either sex, aged 6–11 days and weighing between 4.0 and 8.4 g. Animals were maintained with their litter mates under light–dark cycles of 12 h, at a temperature of 21 ± 2ºC and humidity of 55 ± 15%. All procedures were carried out following European Union and Spanish Government regulations on animal handling, were approved by the local ethics committee and the regional government of Madrid (Ref. PROEX 018/16 and PROEX 51.0/20) and comply with ARRIVE guidelines.

2.1 | Induction of inflammation

Experiments were performed using spinal cord preparations obtained from naïve and paw-inflamed mice. Peripheral inflammation was induced by intraplantar injections of carrageenan (3% in saline, 30 μl) in both hind paws. Paw diameter and mechanical withdrawal threshold were measured before and 20 h after carrageenan injection. The withdrawal threshold was defined as the

minimum mechanical force applied with von Frey filaments that elicited a withdrawal response in at least 3 of 5 trials.

2.2 | *In vitro* spinal cord preparations

For this work, longitudinal slices and hemisected cord preparations were used. Each single preparation was used once and considered as an individual observation, no repeated recordings were obtained from the same preparation and only one drug was applied on each preparation. Extraction and conservation procedures have been described before (Rivera-Arconada et al., 2004; Roza et al., 2016). Briefly, mice were anaesthetized with intraperitoneal urethane (2 mg/kg) and the spinal cords were extracted following a dorsal laminectomy. The whole spinal cord was placed on a plate filled with cold artificial cerebrospinal fluid (ACSF at 4ºC) to remove the outer meninges.

For hemisection, cords were gently separated all along the midline isolating left and right sides. Slices containing the superficial laminae of the cord and attached dorsal roots were prepared in a vibratome (400 μm thick).

Preparations were maintained with oxygenated ACSF (95% O_2, 5% CO_2) at room temperature (22 ± 1°C). The composition of ACSF was (mM): NaCl (127), KCl (1.9), KH_2PO4 (1.5), $MgSO_4$ (1.3), $CaCl_2$ (2), $NaHCO_3$ (22), glucose (10) with pH 7.4.

2.3 | Electrophysiological recordings

For hemisected cords, spontaneous activity from primary afferents and motor neurons was recorded by introducing the L4 dorsal and ventral roots into tight fitting glass suction electrodes. When using slices only the L4 dorsal root was recorded. Signals were obtained using a Multiclamp 700A amplifier (Molecular Devices), sampled at 6 kHz and stored for offline analysis using Spike2 software (CED). Recordings from suction electrodes were amplified (×500) and filtered (10 KHz) to obtain DC signals that were digitized and used to study slow depolarizations. Spontaneous depolarizations recorded from dorsal roots (spontaneous dorsal root potentials, S-DRP) are generated by synchronous depolarizations in unidentified primary afferents. Spontaneous depolarizations recorded from ventral roots (spontaneous ventral root potentials, S-VRP) are generated by depolarizations of populations of motor neurons.

This original DC signal was digitally band-pass filtered between 200 and 1200 kHz to obtain an AC signal that allowed recording of fast spikes (Rivera-Arconada et al., 2004). Spikes recorded from dorsal roots correspond to spontaneous dorsal root reflexes (S-DRRs) generated by synchronous firing of primary afferents, which travel in antidromic direction from the spinal cord. Spikes recorded from the ventral root (spontaneous ventral root reflexes, S-VRRs) reflect the synchronous firing of populations of motor neurons. All measurements were taken from 10 min periods of continuous recordings presenting unperturbed spontaneous activity.

2.4 | Histological analysis of spinal cord slices

Slices were immersed in fixative and kept in cooled (4ºC) paraformaldehyde 4% overnight. Then the slice was washed in phosphate buffer, cryoprotected in sucrose, included in gelatine and frozen. Transverse sections of 50 μm were then obtained in a cryostat (Leica CM1950). Sections were stained with 0.1% toluidine blue to visualize the main histological landmarks of the dorsal horn.

2.5 | Drugs and chemicals

ACSF components, carrageenan lambda, UK 14,304 and the synaptic blockers picrotoxin, gabazine and strychnine were purchased from Sigma Aldrich. NBQX and dAP5 were acquired from Alomone Labs. The ACSF was prepared daily. Drugs were dissolved in milliQ water or DMSO as concentrated stocks (1–50 mM) and conserved frozen at −20ºC. Compounds were diluted in ACSF just before use and applied to the entire preparation during periods of 30–60 min to allow for a complete equilibration within the tissue.

2.6 | Measurements

Depolarizations in DC signals were detected using a home-made algorithm that identifies upward deflections and the time at maximum amplitude. This process was manually supervised to avoid inclusion of artefacts. The maximum amplitude from baseline was then measured using spike2 software. For analysis, we only included S-DRP that exceeded 10 μV or S-VRP larger than 20 μV (to avoid the influence of basal potential oscillations present in motor neurons). Time at maximum amplitude and amplitude for each individual depolarization was annotated.

A threshold criterion was used to count S-DRRs and S-VRRs in AC signals. The threshold was set at four times the root mean square value (RMS) of baseline noise. The total number of spikes counted as well as the time point for threshold crossing was annotated for each spike.

2.7 | Data analysis

Relations between S-DRPs and S-VRPs were studied by cross-correlation analysis using Spike2 software. Time at maximum amplitude of S-DRPs was chosen as trigger for correlograms. When a S-VRP occurred in a time window between −80 ms (IQR −88 and −73 ms) and +18 ms (IQR 10 and 25 ms) from the trigger, the two events were classed as time-locked.

The time course for the rising and decay phases of S-DRP and S-VRPs was measured. The whole population of events of the same class (time-locked or independent) was averaged for each individual experiment. Rising phase was measured as the time to change from 10% to 90% of the maximum amplitude of the response. Decay phase was characterized by the time constants obtained by fitting the data to a one or two phase exponential function. Curve fitting was made using GraphPad Prism 7.0 software (GraphPad Software), that calculate the parameters that best adjust the mathematical equation to the data.

It was common to observe S-DRRs immediately preceding S-DRPs. S-DRRs appearing in the 200 ms before the maximum amplitude of each depolarization were classified as associated activity.

Statistical analysis was performed using GraphPad Prism 7.0 software. All data sets were analysed using non-parametric tests and all data are represented as median and interquartile range (IQR, 25th and 75th quartiles). Wilcoxon matched-pairs signed rank test for paired and Mann–Whitney test for unpaired data comparisons were used.

3 | RESULTS

3.1 | Paw inflammation enhances spontaneous activity

Recordings from dorsal and ventral roots obtained from spinal cord preparations *in vitro* showed abundant spontaneous activity in the form of depolarizations and spike firing (Figure 1a,b). In 19 hemisected spinal cords studied, depolarizations in the dorsal root had a median amplitude of 46 μV (IQR 40–60 μV) and a median frequency of 25.9 S-DRP/min (IQR 19.9–35.7 S-DRP/min). Spike firing in the dorsal root occurred both in association and absence of depolarizations, and showed a frequency of 45.5 S-DRR/min (IQR 31.6–63.1 S-DRR/min). In the ventral root, spontaneous activity consisted of depolarizations that showed a median amplitude of 95 μV (IQR 68–114 μV) and a frequency of 50.7 S-VRP/min (IQR 26.2–96.9 S-VRP/min). Spike firing at a frequency of 26.0 S-VRR/min (IQR 20.7–37.1 S-VRR/min) was also observed.

Equivalent recordings were obtained from spinal cords extracted from mice subjected to an experimental inflammation of the hindpaws 20 h prior to cord extraction. The intraplantar injection of carrageenan into the hindpaws produced a significant increase of paw diameter from 2.2 mm (IQR 2.1–2.2) to 2.7 mm (IQR 2.5–2.9; $n = 33$, $p < 0.001$). Mechanical nociceptive threshold assayed with Von Frey filaments was reduced from a median force of 1 g (IQR 0.8–1.2) before to 0.04 g (IQR 0.04–0.07; $n = 33$, $p < 0.001$) after inflammatory treatment, indicating the development of sensitization. Spinal cords extracted from paw-inflamed mice showed an altered spontaneous activity *in vitro*. Both the amplitude and the frequency of S-DRP, as well as the frequency of S-DRR, increased compared to cords obtained from naïve mice (Figure 1c,d). In the ventral root the median amplitude, but not the frequency, of S-VRP was increased, the frequency of S-VRR did not change after paw inflammation (Figure 1e,f).

3.2 | Spontaneous activity in spinal cord slices from naïve and paw-inflamed mice

Dorsal root recordings were also obtained from spinal cord slices containing the dorsal aspect of the spinal cord and the attached dorsal roots. Histological analysis of the preparations used showed that slices included lamina I through to V (see Figure 2). In slices from naïve mice ($n = 10$), values for amplitude (48.5 μV, IQR 39.2–56.5 μV) and frequency of S-DRP (27.7 S-DRP/min, IQR 20.9–34.6 S-DRP/min), as well as firing of S-DRR (36.4 spikes/min, IQR 27.6–57.9 spikes/min) were not statistically different to those obtained from hemisected cord preparations. These results suggest that circuits responsible of dorsal root activity should be contained within the dorsal horn.

In 10 spinal cord slices obtained from mice that had undergone paw inflammation, the activity recorded from the dorsal root was significantly increased compared to slices from naïve mice, indicating that the increase in activity seen after sensitization involves neurons contained within the dorsal horn. The median amplitude of S-DRP (69.5 μV, IQR 60–117.5; $p < 0.001$) and the firing of S-DRR (77.1 S-DRR/min, IQR 57.7–263.6; $p < 0.01$) augmented, although the frequency of S-DRP did not change significantly (32.4 S-DRP/min, IQR 25.4–44.3).

3.3 | Classification and characteristics of spontaneous activity

A more detailed analysis of the recordings allowed identifying that some spontaneous depolarizations in dorsal and

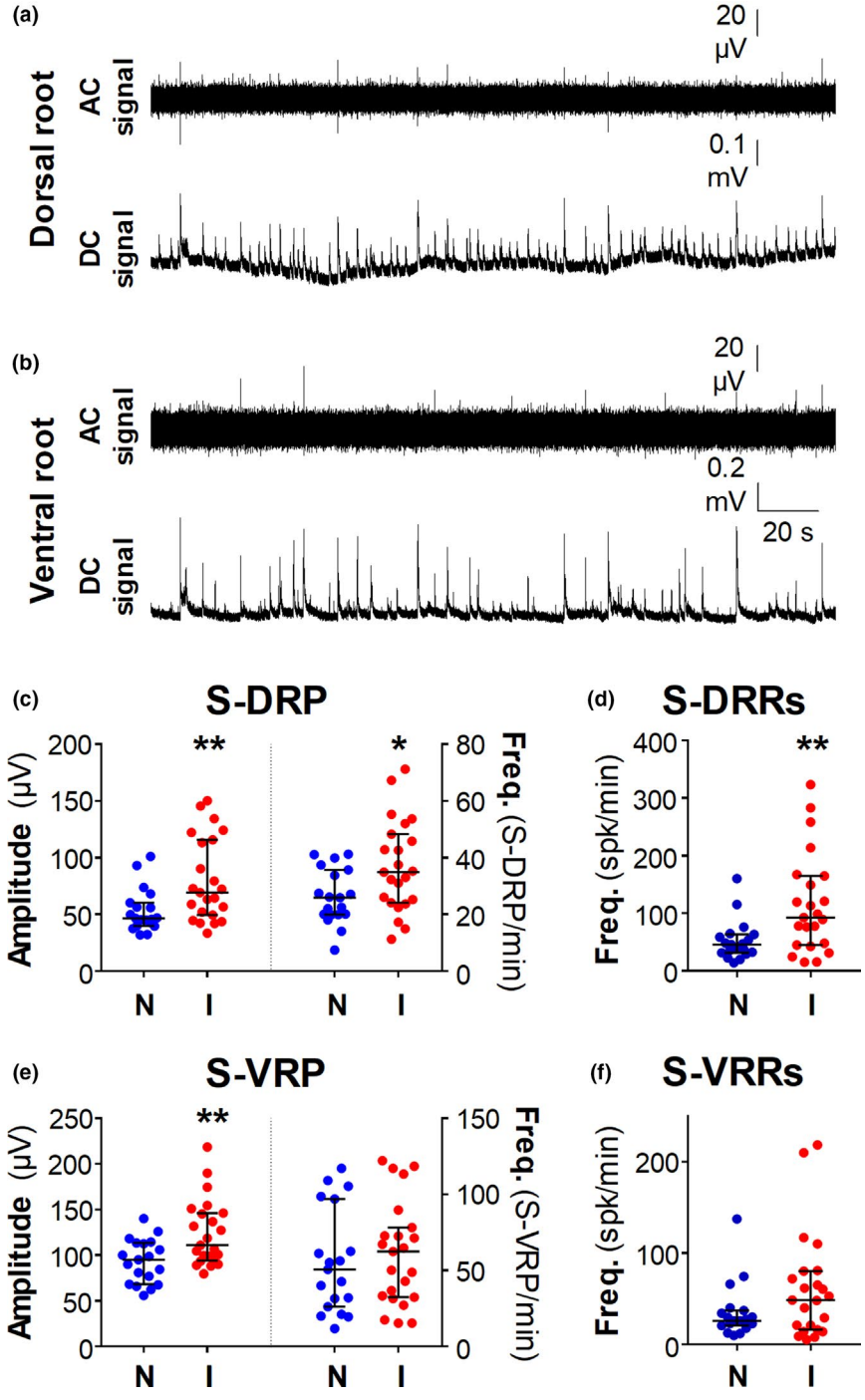

FIGURE 1 Spontaneous activity recorded simultaneously from dorsal and ventral roots in a hemisected spinal cord preparation. Electrophysiological recordings from dorsal (a) and ventral roots (b) showed the spontaneous activity in primary afferent terminals and motor neurons, respectively. Spontaneous activity consisted in slow depolarizations (DC signal) and spike firing (AC signal). Graphs show a quantification of the spontaneous activity in cords from naïve (blue) and paw-inflamed mice (red). In the dorsal root the amplitude and frequency of S-DRP (c) as well as the frequency of S-DRR (d) was increased after inflammation. Graphs in e and f show the equivalent quantification for S-VRP (e) and S-VRR (f). Each data point represents mean values for an individual spinal cord preparation. Interquartile range for each data set is shown superimposed to individual data points. Asterisks indicate statistically significant differences between naïve and paw-inflamed mice (*$p < 0.05$; **$p < 0.01$ Mann–Whitney test).

ventral roots were time-locked, whereas others were independent (Figure 3a–c). In order to study the properties of the different events, we used correlograms (see methods, Figure 3d) to classify them as dorsal root time-locked, ventral root-time locked, dorsal root independent and ventral root independent.

To analyse the temporal relationship between time-locked dorsal and ventral depolarizations, they were averaged and superimposed together with the accumulated number of S-DRRs. This analysis was performed for each experiment (see example on Figure 3e) and the results show that spiking in the dorsal root precedes depolarizations.

Comparing time-locked versus independent S-DRPs, the former had larger amplitude and frequency (Figure 3f,g), but both had similar time course (Table 1). S-DRRs were often associated to time-locked depolarizations (35.3%, IQR 27.3–51.8%) and less commonly to independent ones (5.4% of S-DRR, IQR 2.9–8.5%; $p < 0.001$). There were still a remaining 56.1% S-DRRs (IQR 40.1–66.5%) that occur in the absence of any recorded depolarization. Time-locked S-DRP had a stronger relation to S-DRRs

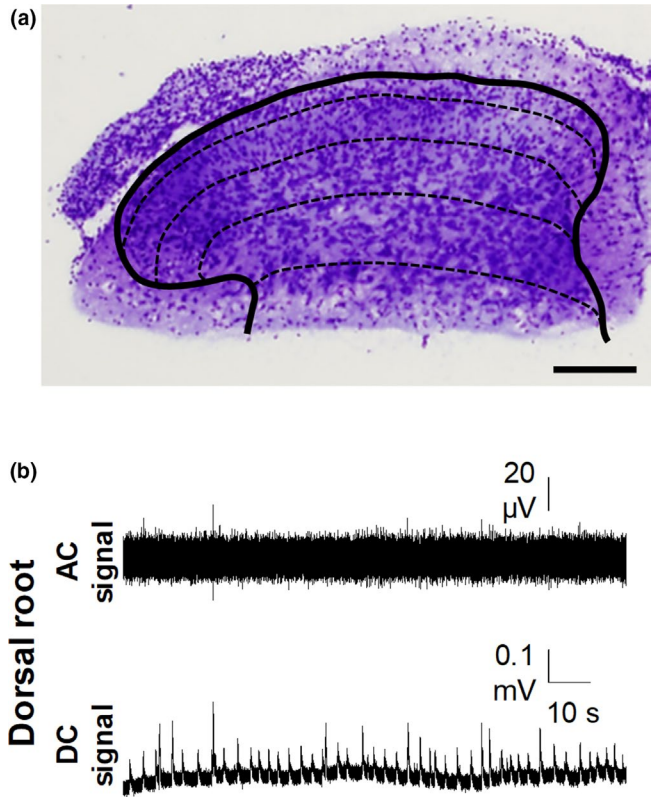

FIGURE 2 Spontaneous activity recorded from spinal cord slices. Photograph in (a) was taken from a transverse section of the spinal cord slice after the staining with 0.1% toluidine blue. Solid lines outline the limits of the white matter and discontinuous lines represent the approximate boundaries of the different laminae. Slices contained the dorsal aspect of the spinal cord, from lamina I to lamina V, and the attached dorsal roots. Calibration bar: 200 μm. Original dorsal root recordings in (b) were obtained from a spinal cord slice. Spontaneous activity showed similar characteristics in comparison with the entire population of events recorded from hemisected cords.

than independent ones (52.0% of depolarizations with firing, IQR 31.8–56.7% vs. 29.4%, IQR 14.4–37.1%, $p < 0.001$) and a larger number of associated spikes (2.06 S-DRR/S-DRP (IQR 1.45–3.17) vs. 1.25 S-DRR/S-DRP, IQR 1.00–1.52; $p < 0.001$).

In the ventral root, comparison between time-locked and independent S-VRPs showed that the first had a larger amplitude but both had similar frequency (Figure 3h,i). These two types of events had also different kinetics (Table 1) with time-locked depolarizations showing longer rising and decay times.

In general terms, cords from paw-inflamed mice showed an enhanced spontaneous activity that reflected in significant changes in several parameters, as summarized in Figure 3. In the dorsal root, all S-DRPs had larger amplitude than their respective controls whereas frequency increased only in independent S-DRPs (Figure 3f,g). Rising and decay phases of S-DRP did not change because of the inflammatory insult. Similarly, S-DRRs showed larger frequency in the treated group, showing an increase in spikes per depolarization, which affected to time-locked (3.22 S-DRR/S-DRP, IQR 2.09–4.98; $p < 0.05$) and independent events (1.45 S-DRR/S-DRP, IQR 1.21–1.85; $p < 0.05$). However, the percentage of S-DRRs that occur associated or in the absence of any depolarization did not change.

In the ventral root, both time-locked and independent depolarizations increased in amplitude compared to cords from naïve mice, with no change in frequency or kinetics (Figure 3h,i).

These results indicate that different types of spontaneous depolarizations can be recorded from both roots and may represent the output of different spinal circuits. Central sensitization may differentially affect these circuits.

3.4 | Pharmacological characterization of spontaneous activity

Pharmacological assays were carried out to define the implication of the main neurotransmitter´ systems in generating spontaneous activity in the spinal cord. Depolarization in dorsal and ventral roots were abolished after the blockade of non-NMDA receptors with 5 μM NBQX ($n = 8$),

FIGURE 3 Characteristics of time-locked and independent depolarizations in both dorsal and ventral roots in cords from naïve and paw-inflamed mice. Original recordings exemplify the different classes of depolarizations studied. Some depolarizations were recorded simultaneously in both roots (a) and were classified as time-locked depolarizations. Note the S-DRRs associated with the depolarizations in AC signal. In both dorsal (b) and ventral root recordings (c) was possible to observe independent depolarizations. Graph in (d) shows a cross correlogram between the time at maximum deflection for S-DRP and the occurrence of S-VRPs from a representative experiment. A clear peak indicative of the existence of correlated activity was observed at ≈ −25 ms. Bin size for cross correlogram is 5 ms. Graph (e) includes the averaged shape of time-locked depolarizations in dorsal and ventral roots as obtained from a representative experiment. In addition, S-DRR counts accumulated for the total period of analysis are included (bin size 5 ms). All events are aligned to the maximum depolarization in S-DRP. S-DRRs were concentrated forming a peak that precedes the rising phase of depolarizations. Graphs f-i show a quantification of mean amplitude (f, h) and frequency (g, i) of depolarizations in dorsal and ventral roots as recorded from hemisected spinal cord preparations obtained from naïve ($n = 19$) and paw-inflamed mice ($n = 23$). Values include data for the depolarizations after the classification in time-locked (diamonds) and independent events ("Indep.", triangles). Asterisks stand for statistically significant differences between naïve and paw-inflamed mice obtained using Mann–Whitney test (*$p < 0.05$; **$p < 0.01$; ***$p < 0.001$).

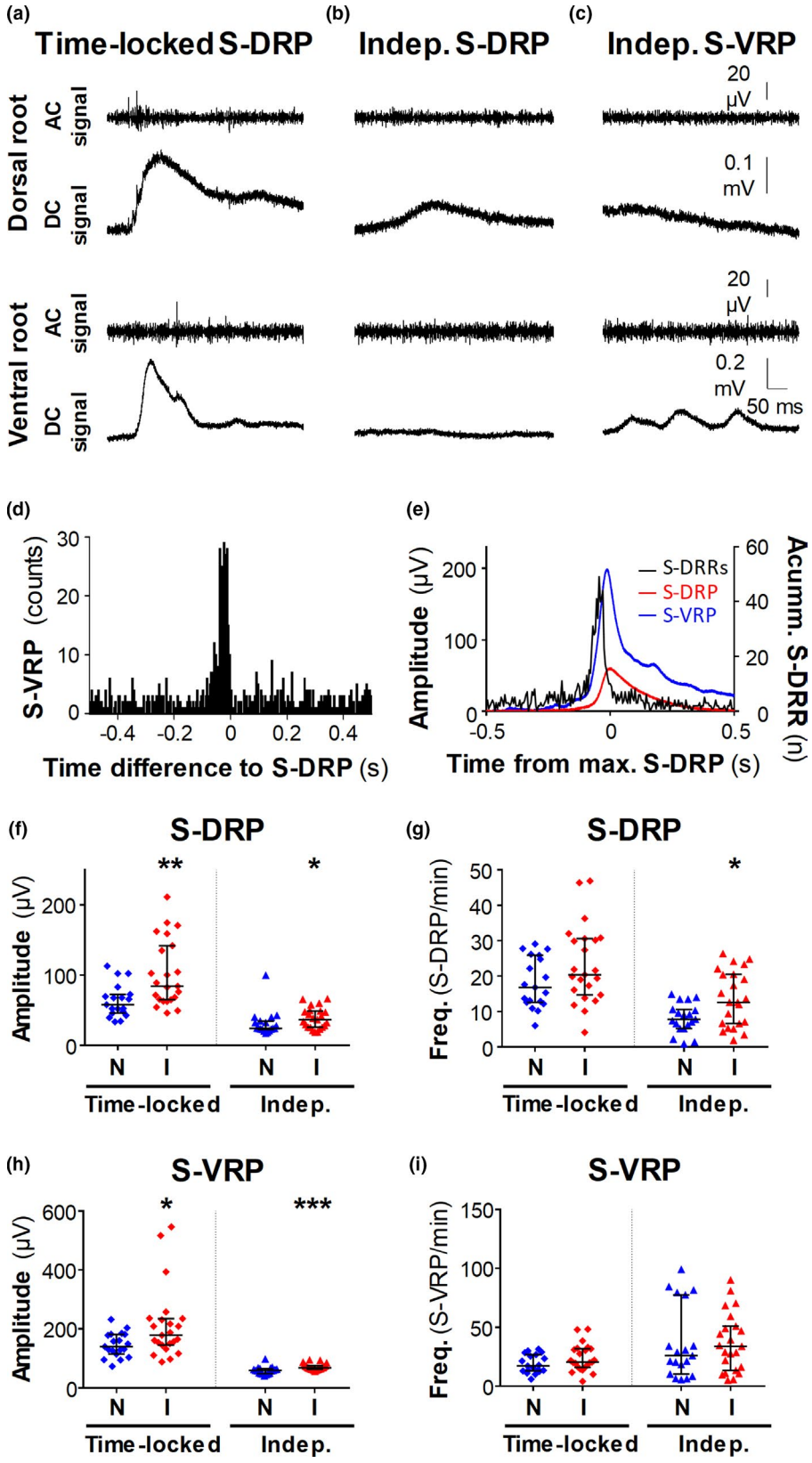

indicating their synaptic origin (Figure 4a). Bursts of S-DRR and S-VRR that occurred in association to depolarizations were absent after NBQX, but some background activity was still present.

Blockade of NMDA receptors with 50 µM dAP5 showed depressant effects on spontaneous activity recorded from both roots (n = 10, Figure 4b). In the dorsal root the frequency of all S-DRPs and the amplitude of time-locked

TABLE 1 Rising and decay kinetics of time-locked and independent depolarizations recorded in dorsal and ventral roots

	10–90% rise time (ms)	Decay time constant (ms)
Dorsal root		
Time-locked S-DRP	85 (75–102)	185 (151–270)
Independent S-DRP	99 (66–108)	218 (141–359)
Ventral root		
Time-locked S-VRP	63 (46–82)	τau1 = 29 (26–38) τau2 = 425 (282–669)
Independent S-VRP	28 (26–31)***	43 (40–57)

Note: Asterisks stand for statistically significant differences obtained using Wilcoxon matched-pairs signed rank test between 10 and 90% rising values for time-locked and independent S-VRP.

***$p < 0.001$.

S-DRPs were significantly reduced (Table 2). The frequency of S-DRR was significantly reduced as well. In the ventral root the amplitude and frequency of S-VRP was depressed. The frequency of S-VRRs were also reduced by dAP5. These results suggest that spontaneous activity depends on neuronal circuits connected by excitatory glutamatergic synapses acting on both NMDA and non-NMDA receptors.

In addition, dorsal root activity was also dependent on the activation of GABA-A receptors (Figure 4c). Application of 3 μM gabazine ($n = 8$) almost abolished S-DRP, with only few low amplitude depolarizations (0.1–0.7 S-DRP/min) remained in 5 of 8 preparations (see Figure 4c). In addition, gabazine reduced the frequency of S-DRR, eliminating spiking associated to S-DRP.

In contrast, the activity in the ventral root was greatly increased. After gabazine, time-locked depolarizations were virtually absent. Independent S-VRP did not change in amplitude but increased in frequency from 24.4 S-VRP/min in control (IQR 15.6–73.1 S-VRP/min) to 81.1 S-VRP/min after GABA-A blockade (IQR 56.1–175.5 S-VRP/min; $p < 0.01$). The frequency of S-VRR was also increased from 31.2 S-VRR/min (IQR 17.3–66.0 S-VRR/min) to 148.4 S-VRR/min (IQR 54.8–553.1 S-VRR/min; $p < 0.01$) by gabazine. The same pattern of effects was observed with 20 μM picrotoxin ($n = 5$). These experiments indicate that GABAergic activity onto primary afferents is dependent on GABA-A receptors, and that ventral root activity originates from spontaneous circuits controlled by inhibitory neurons.

Application of 1 μM strychnine to block glycinergic transmission produced an increase in the amplitude of time-locked S-DRP from 52 μV (IQR 35–58 μV) to 71 μV (IQR 58–85 μV; $p < 0.05$) and reduced the frequency of independent S-DRPs from 52 S-DRP/min (IQR 14–92) to 19 S-DRP/min (IQR 3–42; $p < 0.05$; Figure 4d). The frequency of S-DRR was not altered by strychnine.

TABLE 2 Summary of the effects of 50 μM dAP5 on spontaneous activity recorded from dorsal and ventral roots in eight spinal cord preparations from naïve mice

	Control	dAP5 (50 μM)
Dorsal root		
Time-locked S-DRP		
Amplitude (μV)	59 (52–79)	32 (25–63)*
Frequency (1/min)	8.8 (4.8–17.0)	1.5 (0.2–2.7)**
Indep. S-DRP		
Amplitude (μV)	35 (24–44)	22 (19–26)
Frequency (1/min)	7.0 (1.5–12.3)	2.8 (0.3–6.9)*
S-DRR		
Frequency (1/min)	18.2 (11.2–59.5)	13.3 (8.1–40.0)**
Ventral root		
Time-locked S-VRP		
Amplitude (μV)	165 (125–207)	70 (46–136)**
Frequency (1/min)	9.0 (4.9–17.4)	1.5 (0.2–2.7)**
Indep. S-VRP		
Amplitude (μV)	57 (48–64)	44 (35–59)**
Frequency (1/min)	25.3 (6.8–67.9)	4.1 (2.3–13.0)*
S-VRR		
Frequency (1/min)	16.9 (11.6–29.2)	10.8 (6.5–14.7)**

Note: Median (IQR) frequency and amplitude of events are included for the events classified as dorsal and ventral time-locked and independent (Indep.). Median (IQR) frequency of S-DRR and S-VRR is also included. Asterisks stand for statistically significant differences obtained using Wilcoxon matched-pairs signed rank test between values in control conditions and after dAP5 application.

*$p < 0.05$; **$p < 0.01$.

In the ventral root, both types of S-VRP augmented in amplitude after strychnine, for time-locked from 179 μV (IQR 115–204) to 384 μV (IQR 298–792; $p < 0.05$) and for independent depolarizations from 66 μV (IQR 50–68) to 83 μV (IQR 71–89; $p < 0.05$). S-VRR increased from 40.0 spikes/min (IQR 17.9–74.5) to 101.1 spikes/min (IQR 82.1–141.4; $p < 0.05$). Often, profuse spiking associated to depolarizations.

Blocking glycine receptors seems to have less influence on rhythmicity, but potentiates the amplitude of the spontaneous activity, principally in the ventral root.

3.5 | Modulation of spontaneous activity by the α2-adrenergic agonist UK 14,304

Finally, we wanted to explore the influence of the descending adrenergic system in the spontaneous activity observed in dorsal and ventral roots. Adrenergic modulation

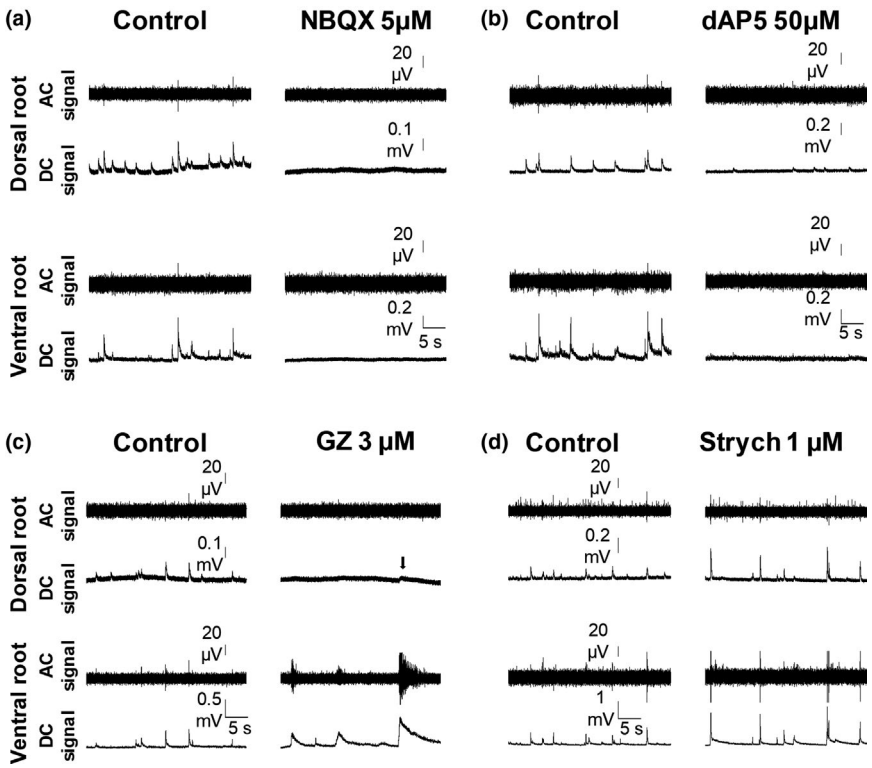

FIGURE 4 Pharmacology of spinal circuits responsible for spontaneous activity. Figures show simultaneous recordings from dorsal and ventral roots obtained from naïve mice before (Control) and after drug application. The non-NMDA receptor blocker NBQX at 5 μM depressed spontaneous activity abolishing depolarizations (a). Blockade of NMDA receptors with dAP5 (50 μM) also reduced spontaneous activity (b). Application of the GABA-A receptor antagonist gabazine (GZ, 3 μM) produced a profound depressant effect on dorsal root activity, but showed excitatory actions in the ventral root (c). Arrow point at one of the few small depolarizations that can be detected in the dorsal root during gabazine application. Recordings in (d) show the excitatory effects of strychnine (Strych, 1 μM), an antagonist of glycine receptors, on the activity recorded from both roots.

is determinant for spinal cord processing of nociceptive information and the activation of α2-adrenergic receptors at the spinal level has analgesic effects.

In naïve animals, the application of the α2-adrenergic agonist UK 14,304 produced a depression of spontaneous activity in dorsal and ventral roots (see Table 3). The median frequency and amplitude of time-locked S-DRP was significantly reduced. In contrast, independent S-DRP were not affected by UK 14,304. S-DRR frequency was significantly depressed. In the ventral root, frequency of both types of depolarizations was strongly reduced without changing their median amplitude. No effects were observed on the frequency of S-VRR.

In spinal cord preparations obtained from paw-inflamed mice, UK 14,304 also reduced the frequency of time-locked S-DRP and S-DRR (Table 3). However, effects of UK 14,304 on the amplitude of S-DRP showed some differences between naïve and paw-inflamed mice. Contrary with the actions observed in naïve, UK 14,304 failed to depress the amplitude of time-locked S-DRP. In addition, the amplitude of independent S-DRP was significantly increased. In the ventral root, UK 14,304 showed the same effects observed in naïve mice. These results indicate that adrenergic transmission may regulate spontaneous activity in the spinal cord, in addition the modulation of S-DRP may change during central sensitization.

4 | DISCUSSION

4.1 | Changes in spontaneous activity after peripheral inflammation

In this study, we show that spontaneous activity in the dorsal and ventral roots is modified by a peripheral inflammatory insult, which highlights a novel component of central sensitization. This effect is preserved in slices containing only the dorsal horn, which indicates that it is produced in sensory areas of the cord. The inflammatory insult produced signs of sensitization in the behaving animal, as was reported on previous occasions (Hedo et al., 1999; Rivera-Arconada & Lopez-Garcia, 2010). Moreover, the amplitude and frequency of DRPs, the experimental correlate of PAD, was significantly augmented on the isolated spinal cord under inflammatory conditions. Several mechanisms for the enhanced PAD during

TABLE 3 Summary of the effects of 0.1 μM UK 14,304 on spontaneous activity recorded from dorsal and ventral roots in cords from seven naïve and seven paw-inflamed mice

	Naïve		Paw-Inflamed	
	Control	**UK (0.1 μM)**	**Control**	**UK (0.1 μM)**
Dorsal root				
Time-locked S-DRP				
Amplitude (μV)	67.8 (52.7–102.4)	31.0 (25.3–47.2)*	100.4 (63.0–159.0)	93.1 (40.7–107.1)
Frequency (1/min)	19.7 (12.9–27.8)	0.4 (0.1–0.8)*	19.9 (13.8–30.8)	2.1 (0.3–4.1)*
Indep. S-DRP				
Amplitude (μV)	23.6 (21.2–40.3)	23.8 (12.7–41.8)	32.3 (26.0–44.1)	67.5 (36.9–74.4)*
Frequency (1/min)	7.8 (7.1–10.6)	2.4 (1.0–8.8)	7.1 (5.3–24.8)	9.6 (6.5–11.7)
S-DRR				
Frequency (1/min)	48.1 (39.2–75.7)	9.5 (7.9–14.7)*	76.3 (42.6–283.1)	21.2 (8.5–60.9)*
Ventral root				
Time-locked S-VRP				
Amplitude (μV)	129.6 (126.6–181.6)	88.3 (67.5–118.2)	187.8 (161.3–257.6)	127.6 (63.3–192.2)
Frequency (1/min)	21.4 (13.6–29.1)	0.4 (0.1–0.8)*	20.2 (13.8–32.3)	2.2 (0.3–4.3)*
Indep. S-VRP				
Amplitude (μV)	59.8 (51.4–62.9)	64.0 (45.0–83.7)	68.5 (65.9–85.4)	71.1 (52.9–76.4)
Frequency (1/min)	21.3 (10.4–34.1)	0.5 (0.1–0.7)*	29.1 (16.4–68.6)	0.6 (0.5–1.4)*
S-VRR				
Frequency (1/min)	24.5 (22.8–29.7)	16.9 (16.2–25.6)	52.9 (21.0–71.9)	40.3 (10.2–52.6)

Note: Median (IQR) frequency and amplitude of events are included for the events classified as time-locked and independent (Indep.). Median (IQR) frequency of S-DRR and S-VRR is also included. Asterisks stand for statistically significant differences obtained using Wilcoxon matched-pairs signed rank test between values in control conditions and after UK 14,304 application.

*$p < 0.05$.

inflammation have been proposed. Previous studies have shown increased GABAergic currents in afferent neurons (Zhu et al., 2012), increased activity of NKCC1 transporters (Price et al., 2009), reduced potassium currents in DRG neurons and depolarization-induced activation of low voltage-activated Ca^{2+} currents (Zhu et al., 2012). In addition, the frequency of DRRs was significantly higher after inflammation. This observation is consistent with previous reports showing backfiring on primary afferent neurons, including nociceptive ones, in live adult rats, cats and monkeys after inflammation (Lin et al., 2000; Sluka et al., 1995). We observed that motor neurons enhanced subthreshold activity, reflecting an increased synaptic input that may alter their excitability. In this context, increased responses to afferent stimulation have been reported under *in vivo* and *in vitro* conditions (Hedo et al., 1999; Woolf, 1983). Given their characteristics, the *in vitro* preparations constitute an excellent model for the study of the mechanisms of sensitization at a cellular and circuit level.

In isolation from peripheral receptors and superior centres, it would be expected that spontaneously active neurons in the spinal cord would constitute the source of excitation to the circuits mediating PAD. Several groups have reported the presence of spontaneous activity in spinal cord neurons *in vitro* and *in vivo* (Li & Baccei, 2011; Lucas-Romero et al., 2018; Luz et al., 2014; Roza et al., 2016; Sandkuhler & Eblen-Zajjur, 1994), and the local circuits involved in the control of afferent excitability include neurons with spontaneous activity (Chavez et al., 2012). Furthermore, under pathological conditions, the synchrony between spontaneously active neurons may increase (Roza et al., 2016), which may promote the activation of pathways generating PAD (Chavez et al., 2012) and subsequently contribute to the augmented output on the dorsal root.

In our study, the observed spiking in primary afferents was considerable in comparison with reports from *in vivo* experiments. This may have been due to factors such as the animal's age and the recording temperature (Bagust et al., 1989; Brooks et al., 1955; Sluka et al., 1995). During postnatal development, the proportion of neurons with intrinsic firing may be reduced (Li & Baccei, 2011), and there is a maturation of the descending control system (Schwaller

et al., 2016), which likely reduces the occurrence of spontaneous activity. Additionally, cooling the cord may enhance the excitatory actions of spinal neurons, promoting the appearance of dorsal root activity (Brooks et al., 1955).

4.2 | Spinal circuits mediating spontaneous activity of dorsal and ventral roots

Our results suggest the existence of different generators for the spontaneous activity recorded. The simultaneous recordings from dorsal and ventral roots showed events that were clearly time-locked, suggesting a common generator mechanism. In the dorsal root, these were large amplitude depolarizations, which are often associated with spike firing. Our analysis suggests that afferent fibres having functional connectivity to motor neurons, generate depolarization that is recorded from the ventral root (Bos et al., 2011; Duchen, 1986). In contrast, we observed independent S-DRPs with lower amplitude and frequency than time-locked events. Further considering the differential effects of strychnine on both types of S-DRPs, it is possible that different generators promote both types of events in the dorsal root. Moreover, it has been reported that PAD in large-calibre fibres of cutaneous origin is subjected to phase-dependent modulation that is related to the locomotor cycle. This happens through pathways and/or mechanisms that are different to those responsible for PAD when originated by peripheral inputs (Gossard et al., 1990). In addition, it has also been noted that PAD onto identified cutaneous mechanoreceptors of different sensory submodalities may be elicited by separated systems (Schmidt, 1971). The existence of independent circuits with different characteristics governing the excitability of primary afferents may allow for the modulation of different sets of afferents within the context of diverse events.

Further to time-locked S-VRP, ventral roots also showed activity that was independent of dorsal events with characteristic amplitude and time-course. These events require a different generator. As such, collecting on the previous considerations, we propose the existence of several local generator circuits within the cord, which may serve to modulate excitability in different sensory afferents, motor neurons and sensory-motor transmissions. Our results also indicate that generators may be differentially affected by central sensitization since it was only the independent S-DRP that increased in frequency after paw inflammation.

In addition, this variety of spontaneous events in the dorsal root could be generated on different types of afferents. Under the present experimental conditions, it is not possible to establish the nature of the afferents implicated. However, since the spontaneous activity is preserved in a slice containing only the dorsal horn, it is likely that terminals of fine afferents and mechanoreceptors of cutaneous origin may be major contributors (Bernardi et al., 1995; Rudomin et al., 2013). Furthermore, neurons that form presynaptic contacts with proprioceptive afferents have been described in deeper laminae, including the intermediate zone of the spinal cord and motor nuclei (Eccles et al., 1963; Fink et al., 2014; Jankowska et al., 1981). The excitability in different types of cutaneous afferents may be regulated by related but independent circuits, as has been previously suggested (Zimmerman et al., 2019). Since independent S-DRP increased in frequency after inflammation, it is tempting to speculate whether this type of depolarization may involve nociceptive afferents/circuits. However, this is a possibility that will have to be addressed in future studies. Since recording from individual terminals of fine afferents within the cord is technically challenging, other alternatives, such as calcium imaging in specific populations of primary afferents, may be successful (Chen et al., 2014).

4.3 | Pharmacological characterization of the recorded activity

The main mechanism for the depolarization in the afferents is produced by GABAergic interneurons that form axo-axonic contacts with afferent terminals (Barber et al.,1978; Fink et al., 2014). The release of GABA produces PAD, which reduces the efficacy of transmitter release. However, if the threshold is surpassed, then action potentials are fired at the terminal, which propagates in orthodromic and antidromic directions (Willis, 1999). In our study, a blockade of GABA-A receptors abolished the activity in the afferents confirming this mechanism. The increase in ventral root activity is likely due to disinhibition after GABA-A blockade.

The blockade of glutamatergic transmission also suppresses activity in primary afferents. This suggests that local circuit neurons with autogenous spiking provide excitatory input to the GABAergic interneurons contacting primary afferents. The spinal circuits controlling the excitability of afferents not only integrate inputs from neighbouring fibres but also descending commands from the brain (Jimenez et al., 1987). Dorsal root responses elicited by the electrical stimulation of a nearby dorsal root have shown similar pharmacological sensitivity to both the GABAergic and glutamatergic blockade (Rivera-Arconada & Lopez-Garcia, 2006). Here, we also show that spontaneous activity was depressed by the α2-adrenergic receptor agonist UK14,304, indicating its modulation by descending pathways.

At the neonatal age studied here, the main neurotransmitter systems are present and functional in the spinal cord. The expression of different subunits of glutamate receptors has been reported in neonates at similar locations to those in adults, with both AMPA and NMDA receptors participating in excitatory responses (Bardoni et al., 1998; Jakowec et al., 1995; Mahmoud et al., 2020). Both GABA-A and glycine receptors are expressed after birth in the spinal cord, and soon produce fully inhibitory actions (Baccei & Fitzgerald, 2004; Bremner et al., 2006; Koch et al., 2012). Adrenergic receptors are also expressed and functional in neonates (Savola & Savola, 1996; Walker et al., 2005).

An additional observation of the present work is related to the effects of the α2-adrenergic receptor agonist UK14,304 after inflammation. In naïve mice, UK14,304 had profound inhibitory actions on time-locked S-DRP and DRRs. However, after paw inflammation, UK14,304 increased the amplitude of independent S-DRP. Therefore, the function of the descending noradrenergic system may change during chronic pain processes (Omiya et al., 2008; Patel et al., 2018). Furthermore, modifications in the expression of α2-receptors and their functionality have been reported in pain models (Bantel et al., 2005; Birder & Perl, 1999; Chen et al., 2011). The differences observed here may be reflecting an adjustment in the adrenergic system, and may outline a putative implication of presynaptic inhibition in adrenergic analgesia.

In conclusion, the results show that an inflammatory insult can modify the spontaneous activity present in the spinal cord, which enhances the output of the circuits responsible for PAD. Different generators are likely implicated in these responses, which may enable a specific interaction with populations of primary afferent. In addition, the descending adrenergic modulation onto these circuits may be altered by inflammation.

CONFLICTS OF INTEREST

The authors have no financial or non-financial interests to disclose.

AUTHORS' CONTRIBUTIONS

All authors contributed to the conception and design of the work as well as the acquisition, analysis or interpretation of data. Similarly, all authors contributed to draft the work, revised it critically and approved the version to be published.

REFERENCES

Baccei, M. L., & Fitzgerald, M. (2004). Development of GABAergic and glycinergic transmission in the neonatal rat dorsal horn. *Journal of Neuroscience*, *24*, 4749–4757. https://doi.org/10.1523/JNEUROSCI.5211-03.2004

Bagust, J., Kerkut, G. A., & Rakkah, N. I. (1989). The dorsal root reflex in isolated mammalian spinal cord. *Comparative Biochemistry and Physiology, A: Comparative Physiology*, *93*, 151–160. https://doi.org/10.1016/0300-9629(89)90202-8

Bantel, C., Eisenach, J. C., Duflo, F., Tobin, J. R., & Childers, S. R. (2005). Spinal nerve ligation increases alpha2-adrenergic receptor G-protein coupling in the spinal cord. *Brain Research*, *1038*, 76–82. https://doi.org/10.1016/j.brainres.2005.01.016

Barber, R. P., Vaughn, J. E., Saito, K., McLaughlin, B. J., & Roberts, E. (1978). GABAergic terminals are presynaptic to primary afferent terminals in the substantia gelatinosa of the rat spinal cord. *Brain Research*, *141*, 35–55. https://doi.org/10.1016/0006-8993(78)90615-7

Bardoni, R., Magherini, P. C., & MacDermott, A. B. (1998). NMDA EPSCs at glutamatergic synapses in the spinal cord dorsal horn of the postnatal rat. *Journal of Neuroscience*, *18*, 6558–6567. https://doi.org/10.1523/JNEUROSCI.18-16-06558.1998

Bernardi, P. S., Valtschanoff, J. G., Weinberg, R. J., Schmidt, H. H., & Rustioni, A. (1995). Synaptic interactions between primary afferent terminals and GABA and nitric oxide-synthesizing neurons in superficial laminae of the rat spinal cord. *Journal of Neuroscience*, *15*, 1363–1371. https://doi.org/10.1523/JNEUROSCI.15-02-01363.1995

Birder, L. A., & Perl, E. R. (1999). Expression of alpha2-adrenergic receptors in rat primary afferent neurones after peripheral nerve injury or inflammation. *Journal of Physiology*, *515*(Pt 2), 533–542. https://doi.org/10.1111/j.1469-7793.1999.533ac.x

Bos, R., Brocard, F., & Vinay, L. (2011). Primary afferent terminals acting as excitatory interneurons contribute to spontaneous motor activities in the immature spinal cord. *Journal of Neuroscience*, *31*, 10184–10188. https://doi.org/10.1523/JNEUROSCI.0068-11.2011

Boyle, K. A., Gradwell, M. A., Yasaka, T., Dickie, A. C., Polgar, E., Ganley, R. P., Orr, D. P. H., Watanabe, M., Abraira, V. E., Kuehn, E. D., Zimmerman, A. L., Ginty, D. D., Callister, R. J., Graham, B. A., & Hughes, D. I. (2019). Defining a spinal microcircuit that gates myelinated afferent input: Implications for tactile allodynia. *Cell Reports*, *28*, 526–540.e6. https://doi.org/10.1016/j.celrep.2019.06.040

Bremner, L., Fitzgerald, M., & Baccei, M. (2006). Functional GABA(A)-receptor-mediated inhibition in the neonatal dorsal horn. *Journal of Neurophysiology*, *95*, 3893–3897. https://doi.org/10.1152/jn.00123.2006

Brooks, C. M., Koizumi, K., & Malcolm, J. L. (1955). Effects of changes in temperature on reactions of spinal cord. *Journal of Neurophysiology*, *18*, 205–216. https://doi.org/10.1152/jn.1955.18.3.205

Cervero, F., & Laird, J. M. (1996). Mechanisms of touch-evoked pain (allodynia): a new model. *Pain*, *68*, 13–23. https://doi.org/10.1016/S0304-3959(96)03165-X

Chavez, D., Rodriguez, E., Jimenez, I., & Rudomin, P. (2012). Changes in correlation between spontaneous activity of dorsal horn neurones lead to differential recruitment of inhibitory pathways in the cat spinal cord. *Journal of Physiology*, *590*, 1563–1584. https://doi.org/10.1113/jphysiol.2011.223271

Chen, J. T., Guo, D., Campanelli, D., Frattini, F., Mayer, F., Zhou, L., Kuner, R., Heppenstall, P. A., Knipper, M., & Hu, J. (2014). Presynaptic GABAergic inhibition regulated by BDNF contributes to neuropathic pain induction. *Nature Communications*, *5*, 5331. https://doi.org/10.1038/ncomms6331

Chen, S. R., Chen, H., Yuan, W. X., & Pan, H. L. (2011). Increased presynaptic and postsynaptic alpha2-adrenoceptor activity in the spinal dorsal horn in painful diabetic neuropathy. *Journal of Pharmacology and Experimental Therapeutics*, *337*, 285–292. https://doi.org/10.1124/jpet.110.176586

Dubuc, R., Cabelguen, J. M., & Rossignol, S. (1985). Rhythmic antidromic discharges of single primary afferents recorded in cut dorsal root filaments during locomotion in the cat. *Brain Research*, *359*, 375–378. https://doi.org/10.1016/0006-8993(85)91455-6

Duchen, M. R. (1986). Excitation of mouse motoneurones by GABA-mediated primary afferent depolarization. *Brain Research*, *379*, 182–187. https://doi.org/10.1016/0006-8993(86)90274-x

Eccles, J. C., Schmidt, R. F., & Willis, W. D. (1963). The location and the mode of action of the presynaptic inhibitory pathways on to group I afferent fibers from muscle. *Journal of Neurophysiology*, *26*, 506–522. https://doi.org/10.1152/jn.1963.26.3.506

Fink, A. J., Croce, K. R., Huang, Z. J., Abbott, L. F., Jessell, T. M., & Azim, E. (2014). Presynaptic inhibition of spinal sensory feedback ensures smooth movement. *Nature*, *509*, 43–48. https://doi.org/10.1038/nature13276

French, A. S., Panek, I., & Torkkeli, P. H. (2006). Shunting versus inactivation: simulation of GABAergic inhibition in spider mechanoreceptors suggests that either is sufficient. *Neuroscience Research*, *55*, 189–196. https://doi.org/10.1016/j.neures.2006.03.002

Gossard, J. P., Bouyer, L., & Rossignol, S. (1999). The effects of antidromic discharges on orthodromic firing of primary afferents in the cat. *Brain Research*, *825*, 132–145. https://doi.org/10.1016/0006-8993(85)91455-6

Gossard, J. P., Cabelguen, J. M., & Rossignol, S. (1990). Phase-dependent modulation of primary afferent depolarization in single cutaneous primary afferents evoked by peripheral stimulation during fictive locomotion in the cat. *Brain Research*, *537*, 14–23. https://doi.org/10.1016/0006-8993(90)90334-8

Guo, D., & Hu, J. (2014). Spinal presynaptic inhibition in pain control. *Neuroscience*, *283*, 95–106. https://doi.org/10.1016/j.neuroscience.2014.09.032

Hedo, G., Laird, J. M., & Lopez-Garcia, J. A. (1999). Time-course of spinal sensitization following carrageenan-induced inflammation in the young rat: a comparative electrophysiological and behavioural study in vitro and in vivo. *Neuroscience*, *92*, 309–318. https://doi.org/10.1016/s0306-4522(98)00734-9

Jakowec, M. W., Yen, L., & Kalb, R. G. (1995). In situ hybridization analysis of AMPA receptor subunit gene expression in the developing rat spinal cord. *Neuroscience*, *67*, 909–920. https://doi.org/10.1016/0306-4522(95)00094-y

Jankowska, E., McCrea, D., Rudomin, P., & Sykova, E. (1981). Observations on neuronal pathways subserving primary afferent depolarization. *Journal of Neurophysiology*, *46*, 506–516. https://doi.org/10.1152/jn.1981.46.3.506

Jimenez, I., Rudomin, P., & Solodkin, M. (1987). Mechanisms involved in the depolarization of cutaneous afferents produced by segmental and descending inputs in the cat spinal cord. *Experimental Brain Research*, *69*, 195–207. https://doi.org/10.1007/BF00247042

Koch, S. C., Tochiki, K. K., Hirschberg, S., & Fitzgerald, M. (2012). C-fiber activity-dependent maturation of glycinergic inhibition in the spinal dorsal horn of the postnatal rat. *Proceedings of the National Academy of Sciences of the United States of America*, *109*, 12201–12206. https://doi.org/10.1073/pnas.1118960109

Li, J., & Baccei, M. L. (2011). Pacemaker neurons within newborn spinal pain circuits. *Journal of Neuroscience*, *31*, 9010–9022. https://doi.org/10.1523/JNEUROSCI.6555-10.2011

Lin, Q., Zou, X., & Willis, W. D. (2000). Adelta and C primary afferents convey dorsal root reflexes after intradermal injection of capsaicin in rats. *Journal of Neurophysiology*, *84*, 2695–2698. https://doi.org/10.1152/jn.2000.84.5.2695

Lucas-Romero, J., Rivera-Arconada, I., Roza, C., & Lopez-Garcia, J. A. (2018). Origin and classification of spontaneous discharges in mouse superficial dorsal horn neurons. *Scientific Reports*, *8*, 9735-y. https://doi.org/10.1038/s41598-018-27993-y

Luz, L. L., Szucs, P., & Safronov, B. V. (2014). Peripherally driven low-threshold inhibitory inputs to lamina I local-circuit and projection neurones: a new circuit for gating pain responses. *Journal of Physiology*, *592*, 1519–1534. https://doi.org/10.1113/jphysiol.2013.269472

Mahmoud, H., Martin, N., & Hildebrand, M. E. (2020). Conserved contributions of NMDA receptor subtypes to synaptic responses in lamina II spinal neurons across early postnatal development. *Mol Brain*, *13*, 31–39. https://doi.org/10.1186/s13041-020-00566-9

Omiya, Y., Yuzurihara, M., Suzuki, Y., Kase, Y., & Kono, T. (2008). Role of alpha2-adrenoceptors in enhancement of antinociceptive effect in diabetic mice. *European Journal of Pharmacology*, *592*, 62–66. https://doi.org/10.1016/j.ejphar.2008.06.087

Patel, R., Qu, C., Xie, J. Y., Porreca, F., & Dickenson, A. H. (2018). Selective deficiencies in descending inhibitory modulation in neuropathic rats: implications for enhancing noradrenergic tone. *Pain*, *159*, 1887–1899. https://doi.org/10.1097/j.pain.0000000000001300

Price, T. J., Cervero, F., Gold, M. S., Hammond, D. L., & Prescott, S. A. (2009). Chloride regulation in the pain pathway. *Brain Research Reviews*, *60*, 149–170. https://doi.org/10.1016/j.brainresrev.2008.12.015

Rivera-Arconada, I., & Lopez-Garcia, J. A. (2006). Retigabine-induced population primary afferent hyperpolarisation in vitro. *Neuropharmacology*, *51*, 756–763. https://doi.org/10.1016/j.neuropharm.2006.05.015

Rivera-Arconada, I., & Lopez-Garcia, J. A. (2010). Changes in membrane excitability and potassium currents in sensitized dorsal horn neurons of mice pups. *Journal of Neuroscience*, *30*, 5376–5383. https://doi.org/10.1523/JNEUROSCI.4359-09.2010

Rivera-Arconada, I., Martinez-Gomez, J., & Lopez-Garcia, J. A. (2004). M-current modulators alter rat spinal nociceptive transmission: an electrophysiological study in vitro. *Neuropharmacology*, *46*, 598–606. https://doi.org/10.1016/j.neuropharm.2003.10.016

Roza, C., Mazo, I., Rivera-Arconada, I., Cisneros, E., Alayon, I., & Lopez-Garcia, J. A. (2016). Analysis of spontaneous activity of superficial dorsal horn neurons in vitro: neuropathy-induced changes. *Pflugers Archiv. European Journal of Physiology*, *468*, 2017–2030. https://doi.org/10.1007/s00424-016-1886-6

Rudomin, P. (1990). Presynaptic inhibition of muscle spindle and tendon organ afferents in the mammalian spinal cord. *Trends in Neurosciences*, *13*, 499–505. https://doi.org/10.1016/0166-2236(90)90084-n

Rudomin, P., Jimenez, I., & Chavez, D. (2013). Differential presynaptic control of the synaptic effectiveness of cutaneous afferents evidenced by effects produced by acute nerve section. *Journal of Physiology*, *591*, 2629–2645. https://doi.org/10.1113/jphysiol.2013.253351

Rudomin, P., & Schmidt, R. F. (1999). Presynaptic inhibition in the vertebrate spinal cord revisited. *Experimental Brain Research*, *129*, 1–37. https://doi.org/10.1007/s002210050933

Sandkuhler, J., & Eblen-Zajjur, A. A. (1994). Identification and characterization of rhythmic nociceptive and non-nociceptive spinal dorsal horn neurons in the rat. *Neuroscience*, *61*, 991–1006. https://doi.org/10.1016/0306-4522(94)90419-7

Savola, M. K., & Savola, J. M. (1996). alpha 2A/D-Adrenoceptor subtype predominates also in the neonatal rat spinal cord. *Brain Research. Developmental Brain Research*, *94*, 106–108. https://doi.org/10.1016/0165-3806(96)00060-0

Schmidt, R. F. (1971). Presynaptic inhibition in the vertebrate central nervous system. *Ergebnisse Der Physiologie*, *63*, 20–101. https://doi.org/10.1007/BFb0047741

Schwaller, F., Kwok, C., & Fitzgerald, M. (2016). Postnatal maturation of the spinal-bulbo-spinal loop: brainstem control of spinal nociception is independent of sensory input in neonatal rats. *Pain*, *157*, 677–686. https://doi.org/10.1097/j.pain.0000000000000420

Sluka, K. A., Rees, H., Westlund, K. N., & Willis, W. D. (1995). Fiber types contributing to dorsal root reflexes induced by joint inflammation in cats and monkeys. *Journal of Neurophysiology*, *74*, 981–989. https://doi.org/10.1152/jn.1995.74.3.981

Walker, S. M., Howard, R. F., Keay, K. A., & Fitzgerald, M. (2005). Developmental age influences the effect of epidural dexmedetomidine on inflammatory hyperalgesia in rat pups. *Anesthesiology*, *102*, 1226–1234. https://doi.org/10.1097/00000542-200506000-00024

Willis, W. D. (1999). Dorsal root potentials and dorsal root reflexes: a double-edged sword. *Experimental Brain Research*, *124*, 395–421. https://doi.org/10.1007/s002210050637

Woolf, C. J. (1983). Evidence for a central component of post-injury pain hypersensitivity. *Nature*, *306*, 686–688. https://doi.org/10.1038/306686a0

Zhu, Y., Dua, S., & Gold, M. S. (2012). Inflammation-induced shift in spinal GABA(A) signaling is associated with a tyrosine kinase-dependent increase in GABA(A) current density in nociceptive afferents. *Journal of Neurophysiology*, *108*, 2581–2593. https://doi.org/10.1152/jn.00590.2012

Zhu, Y., Lu, S. G., & Gold, M. S. (2012). Persistent inflammation increases GABA-induced depolarization of rat cutaneous dorsal root ganglion neurons in vitro. *Neuroscience*, *220*, 330–340. https://doi.org/10.1016/j.neuroscience.2012.06.025

Zimmerman, A. L., Kovatsis, E. M., Pozsgai, R. Y., Tasnim, A., Zhang, Q., & Ginty, D. D. (2019). Distinct modes of presynaptic inhibition of cutaneous afferents and their functions in behavior. *Neuron*, *102*, 420–434.e8. https://doi.org/10.1016/j.neuron.2019.02.002

How to cite this article: Vicente-Baz, J., Lopez-Garcia, J. A., & Rivera-Arconada, I. (2022). Central sensitization of dorsal root potentials and dorsal root reflexes: An in vitro study in the mouse spinal cord. *European Journal of Pain*, 26, 356–369. https://doi.org/10.1002/ejp.1864